Oncology
and Radiotherapy©
19(11) 2025 : 001-009 • RESEARCH ARTICLE

Evaluation of the impact of slice thickness on CT and Cone Beam CT image quality in radiotherapy

Amine El Outmani[1,2]*, M. Zerfaoui[1], I. Hattal[1,2], A. Rrhioua[1], D. Bakari[3], Y. Oulhouq[1], K. Bahhous[5]

[1]Mohammed First University, Faculty of Sciences, LPTPME, Oujda, Morocco
[2]Centre Oriental Al Kindy, Oncologie et diagnostic du Maroc (ODM), Oujda, Morocco
[3]National School of Applied Sciences, University Mohammed First, Oujda, Morocco
[4]Faculty of Medicine and pharmacy, Mohammed First University, Oujda, Morocco

ABSTRACT

Objective: This study evaluates the accuracy of slice thickness and its impact on CT and Cone Beam CT (CBCT) image quality and dose distribution in radiotherapy.

Materials and Methods: The Catphan 604 phantom was scanned using a CT scanner and a linear accelerator On-Board Imager. Images were acquired at 1, 3, and 5 mm slice thicknesses to assess the effects on low-contrast resolution, Hounsfield Unit (HU), Modulation Transfer Function (MTF), uniformity, and Contrast-to-Noise Ratio (CNR). Analysis and dose calculation were performed using Pylinac and Eclipse, respectively.

Results: Greater measurement errors were detected for CBCT slice thickness compared to CT. Thinner slices improved resolution but increased noise, whereas thicker slices reduced noise but compromised detail. CT outperformed CBCT in terms of resolution, HU accuracy, uniformity, and CNR. Slice thickness had no significant effect on dose distribution, but differences were noted in bone structures between the modalities.

Conclusion: Slice thickness significantly affects CT and CBCT image quality. Its verification is essential for optimizing radiotherapy imaging protocols.

Keywords: CT; CBCT; Slice Thickness; Image Quality; Radiotherapy

Address for correspondence:
Amine El Outmani
Mohammed First University, Faculty of Sciences,
LPTPME, Oujda, Morocco
E-mail: am.eloutmani@ump.ac.ma

Word count: 3622 **Tables:** 04 **Figures:** 08 **References:** 27

Received: 07 Oct, 2025, Manuscript No. OAR-25-171673;
Editor assigned: 10 Oct, 2025, PreQC No. OAR-25-171673 (PQ);
Reviewed: 22 Oct, 2025, QC No. OAR-25-171673;
Revised: 03 Nov, 2025, Manuscript No. OAR-25-171673 (R);
Published: 28 Nov, 2025

INTRODUCTION

Computed Tomography (CT) scanning and Cone Beam Computed Tomography (CBCT) have transformed radiotherapy (RT) and medical imaging [1]. These imaging modalities are essential components of clinical workflows and are of critical importance in diagnosis and treatment planning [2]. CT and CBCT images are directly related to the diagnostic interpretation and accuracy of RT treatment [3]. In the field of RT, clear visualization of tumors and surrounding tissues is critical to ensure that radiation is delivered precisely and carefully [4].

Slice thickness is one of the most important factors in determining overall image quality. This parameter has a direct impact on the level of detail encoded in the cross-sectional images and, subsequently, the resolvability of anatomical structures and the fidelity of imaging features [5]. Finding the best slice thickness is important for image quality, which assists in accurate treatment planning [6-8].

The American Association of Physicists in Medicine (AAPM) has established guidelines for slice thickness in RT imaging. For three-dimensional conformal radiotherapy (3D-CRT), AAPM allows slice thicknesses of up to 5 mm [9], while recommending 3 mm for Intensity-Modulated Radiation Therapy (IMRT) and Volumetric Modulated Arc Therapy (VMAT) [10]. For Stereotactic Radiosurgery (SRS) and Stereotactic Radiotherapy (SRT), which demand the highest precision, AAPM suggests a maximum slice thickness of 1 mm [11]. These recommendations are aimed at fine-tuning the slice thickness to confirm the accuracy and efficacy of different RT techniques.

Evaluating and optimizing slice thickness in clinical practice can be challenging owing to limitations in proprietary software and the availability of tools for image quality analysis. Open-source tools represent a good solution, providing flexible and low-cost means of evaluating imaging parameters. These tools allow clinicians and researchers to examine the effects of slice thickness on image quality, which can improve the accuracy and effectiveness of RT.

This study introduced an open-source tool specifically designed to assess the effects of slice thickness on image quality parameters in both CT and CBCT. The methodology aims to compare various

image parameters across different slice thicknesses to determine the optimal balance between preserving essential image details and avoiding unnecessary noise that could degrade image quality. Additionally, the study included a dosimetric analysis comparing dose distributions across various slice thicknesses and between the two imaging techniques.

MATERIALS AND METHODS

Catphan 604

For this study, we employed the Philips Brilliance Big Bore CT scanner and On-Board Imager (OBI) of the Varian Vital beam linear accelerator. Images of the Catphan 604 phantom [12], which contains inserts representing the components of human tissue from the air cavities to the bone, were obtained using a CT scanner. CBCT images were obtained using the OBI device [Figure 1]. The measurements were performed for images acquired using the CT head and neck imaging protocol and the CBCT head and neck protocol. Catphan 604 contains four modules: CTP732: Resolution Geometry Module; CTP682: Sensitometer (CT Number Linearity) Module, CTP730 Low-Contrast Module, and CTP729: Uniformity Module. Both CT and CBCT modalities were used to scan the phantom and the obtained data were analyzed to assess the effect of slice thickness on the image quality in the respective systems.

Pylinac

Images of the Catphan 604 phantom were analyzed using the open-source Python library Pylinac (version 3.25.0) [13], which analyze imaging systems for RT quality assurance (QA). This robust tool facilitates the analysis of datasets and images and can process raw data or images as input data to generate outputs in the form of numerical values, PDFs, graphical, and visualization reports. Pylinac allows medical physicists to quickly confirm that their therapy equipment is working correctly and safely, freeing up precious time and resources in QA workflow. In this study, the relevant Pylinac modules were used for CT and CBCT image analyses. The following parameters were analyzed: slice thickness, Low-Contrast Resolution, Hounsfield Unit (HU), Modulation Transfer Function (MTF), Uniformity and Contrast-to-Noise Ratio.

Slice thickness

Slice thickness is an important parameter because it directly affects the partial volume effect, which occurs when a voxel encompasses different tissues. This can compromise image accuracy and, therefore, treatment precision, especially for small or complicated target volumes such as tumors. In this study, slice thickness was measured at the center of the Field Of View (FOV) as the distance between two points at half the maximum height of the slice profile along the axis of rotation, using the Catphan 604 phantom and Pylinac software.

Low-Contrast Resolution

A low-contrast resolution indicates the system's ability to differentiate between areas with low-density varia-tions. Good low-contrast resolution is particularly important in RT, where accurate delineation of organs at risk and target volumes is the first step for accurate treatment delivery. In this study, the CTP730 module of Catphan 604 was used to measure the low-contrast resolution

Hounsfield Unit (HU)

The critical importance of consistent and reliable Hounsfield Unit (HU) values in RT lies in their role in dose calculation. Improving the HU accuracy in treatment planning maximizes patient benefits. To measure HU in CT and CBCT and identify the difference between the two, the Catphan 604 sensitometry module (CTP682), specifically designed to verify the HU accuracy, was used.

Modulation Transfer Function (MTF)

The modulated transfer function (MTF) is a crucial parameter that indicates the capacity of an imaging system to reproduce fine details while preserving the contrast. In this study, high-resolution inserts of the Catphan 604 phantom were used to evaluate how well the system resolved fine structures under varying contrast conditions. The MTF curves were generated using Pylinac software.

Uniformity

The Uniformity Index (UI) measures the disparity in Hounsfield Unit (HU) values between the peripheral and central Region Of

Figure 1: Catphan 604 Phantom setup with CT scanner and OBI for CT and CBCT images acquisition.

Interest (ROI)of CT or CBCT images and is a crucial tool for evaluating spatial uniformity. It is defined as.

$$UI = \frac{S_{ROIper} - S_{ROIcen}}{S_{ROIper} + 1000} \times 100 \quad \text{Eq. (1)}$$

Where:

UI: uniformity index

S_{ROIper} is the HU value in the peripheral region of interest (ROI) of the image.

S_{ROIcen} is the HU value in the central region of interest (ROI) of the image.

Hounsfield Units (HUs) were measured in the homogeneous region to evaluate deviations across the different zones of the image (top, bottom, right, left, and center) [Figure 2]. A Region of Interest (ROI) with a diameter of 5 mm was selected for the measurements.

A negative UI value indicates a capping artifact, whereas a positive value indicates a cupping artifact. Values near zero indicate a uniform image with minimal artifacts.

Contrast-to-Noise Ratio

The contrast-to-noise ratio (CNR) is an essential quantitative measure for evaluating image noise. In Imaging modalities, such as CT and CBCT, noise greatly impairs the identification of close structures of interest, particu-larly in low-contrast regions. The CNR is a measure of the relationship between contrast, which is the difference between two tissues, in Hounsfield (HU) units, and noise, which is the fluctuation around the mean gray level in pixels for a certain region.

In this study, the image quality for CT and CBCT was assessed using CNR values. The Catphan module with low- contrast cylinders was used to calculate the CNR [Figure 3]. Specifically, a cylindrical disk with a diameter of 15 mm and a nominal low contrast of 1.0 % was sampled with a region of interest (ROI) of 7 mm × 7 mm centered on the disk. A second ROI of the same size was positioned in a nearby homogeneous area devoid of structures to measure the image noise [14].

The CNR was computed using Pylinac with the following equation:

$$CNR = \frac{ROI\,(1\%) - ROI\,(bg)}{SD(bg)} \quad \text{Eq. (2)}$$

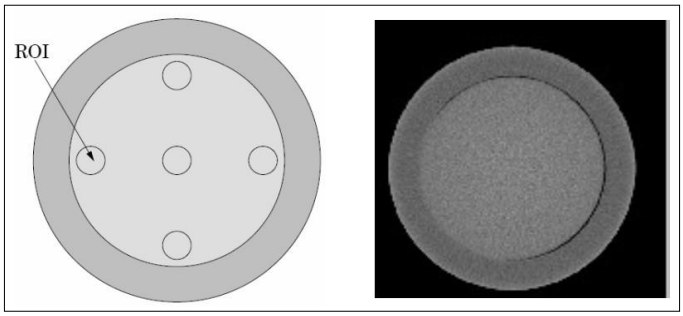

Figure 2: Measurement of uniformity on a CT and CBCT images using the CTP729 module.

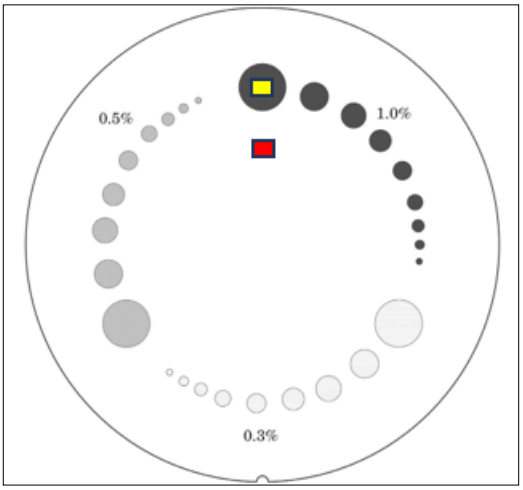

Figure 3: Catphan 604 – Low-Contrast Module (CTP730). The 1.0% low-contrast ROI is shown in yellow, and the background ROI is shown in red.

where ROI(1%) is the mean Hounsfield units (HU) associated with the ROI of a 15-mm diameter, low-contrast disk with 1% as the nominal target contrast level. The ROI(bg) is the mean HU of the area defined as the back-ground, and SD(bg) represents the standard deviation of the background.

RESULTS

Impact of slice thickness on image quality

To examine the influence of slice thickness on CT and CBCT images, image quality was evaluated by compar-ing several factors such as low-contrast resolution, Hounsfield unit (HU), modulation transfer function (MTF), noise, and uniformity.

Control of slice thickness and low-contrast visibility in CT and CBCT images

Analysis of CT and CBCT images using Pylinac software revealed minor discrepancies in the order of a few micrometers between the programmed and measured thicknesses. The measured slice thicknesses were consist-ently thinner than the programmed slice thicknesses on CBCT than on CT. Furthermore, low-contrast visibility improved with increasing slice thickness and was significantly lower on CBCT than on CT, regardless of the measured slice thickness [Table 1].

Influence on Hounsfield Units (HU)

[Table 2], presents the average HU values of all the components of the CTP732 module in the Catphan 604 phantom, recommended by the manufacturer for CT images. It should be noted that the manufacturer did not provide specific ranges for CBCT data; the CT ranges were used as a reference to roughly estimate the density variations in the CBCT images.

[Figure 4], shows the deviation between the measured HU values and the average values provided by the manu-facturer for each component, depending on the HU of the material. A tolerance of ±40 was adopted to evaluate the HU values.

Table 1: Comparison of Slice Thickness and Low-Contrast Visibility in CT and CBCT images.

Slice Thickness (mm)	CT: Measured Thickness (mm)	CBCT: Measured Thickness (mm)	CT: Low-Contrast Visibility	CBCT: Low-Contrast Visibility
1 mm	0.983	0.977	4.24	3.48
3 mm	2.764	2.477	6.66	6.39
5 mm	4.253	4.216	6.85	6.53

Table 2: Nominal HU for Different Materials given by the manufacturer and used in Catphan 604 phantom.

Materials	Air	PMP	LDPE	Poly	Acrylic	Bone 20%	Delrin	Bone 50%	Teflon
HU Range	-1046: -986	-220: -172	-121: -87	-65: -29	92: 137	211: 263	344: 387	667: 783	941: 1060

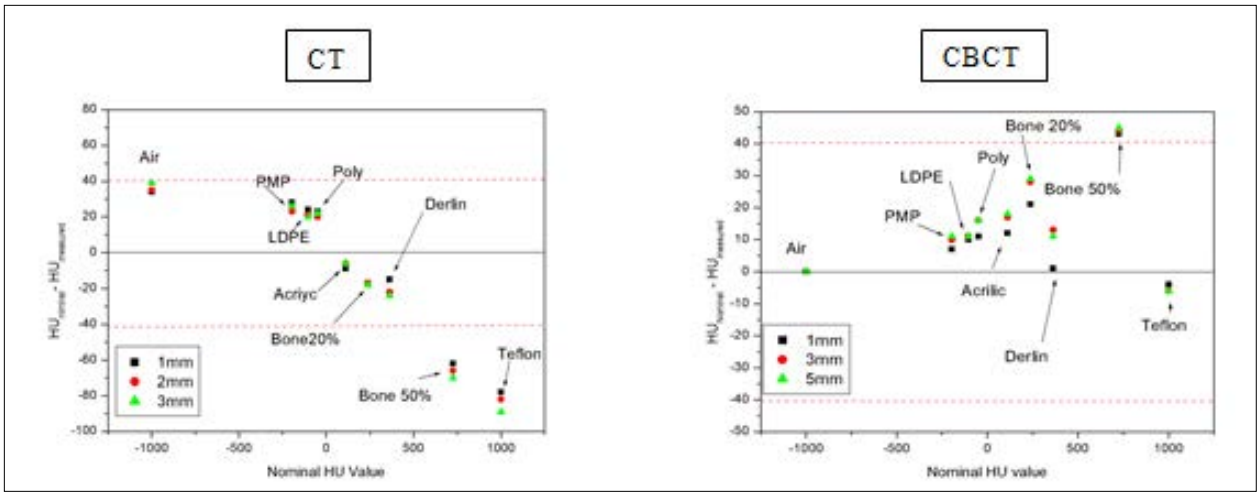

Figure 4: Difference between HU (given by the manufacturer) and measured HU, for different phantom materials, as a function of nominal HU, for slice thicknesses: 1 mm, 3 mm and 5 mm, in the case of CT and CBCT images.

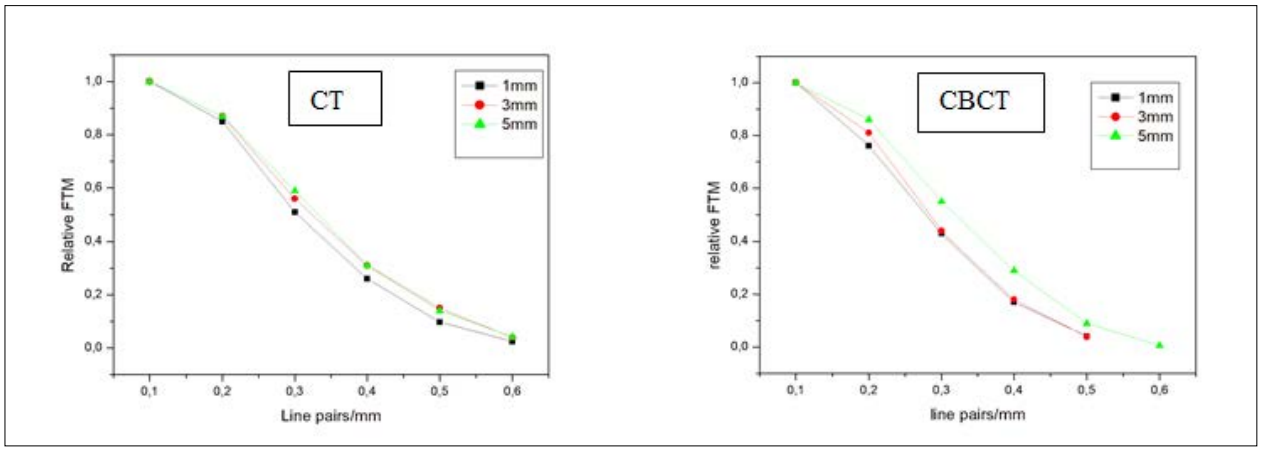

Figure 5: Relative MTF as a function of line pairs per mm (lp/mm) for CT and CBCT images for slice thick-nesses of 1 mm, 3 mm and 5 mm.

The HU values obtained from both the CT and CBCT imaging modalities were virtually identical for each part of the phantom and for all slice thicknesses studied. This indicates the low influence of slice thickness on HU for the same modality. However, a notable difference was observed between the HU values obtained by CBCT and CT. In the CT image, the difference increased as the material became denser. This is particularly noticeable for dense materials, such as Teflon and Bone 50%.

CBCT images also revealed a similar pattern, in which the difference generally increased with density. However, the differences were generally smaller, with only the bone 50% exceeding the acceptable limit. Overall, CBCT showed less variability than CT for the slice thicknesses examined in this study.

Influence on the MTF

[Figure 5], shows how the Modulation Transfer Function (MTF) changes with increasing line pairs per millimeter (lp/mm) for slice

thicknesses of 1, 3, and 5 mm. Although CT and CBCT images follow similar patterns, there are significant differences in their spatial resolutions. The CT images maintained an MTF of up to 6 lp/cm across all slice thicknesses. In contrast, CBCT images only reach up to 5 lp/cm for 1 mm and 3 mm thicknesses. Additionally, the MTF on CBCT decreased more rapidly than that on CT. For both imaging methods, thicker slices provided better resolution than thinner slices. These findings indicate that CT delivers better spatial resolution than CBCT.

Influence on the MTF Influence on Noise and Uniformity

[Table 3], shows noise and uniformity index measurements for CT and CBCT images at three slice thicknesses (1 mm, 3 mm, and 5 mm). Results indicate that CT images demonstrate excellent homogeneity with minimal distortion. In contrast, CBCT images display more variation, with more significant uniformity differences when changing slice thickness from 1 mm to 3 mm. Noise levels are lower in CT images compared to CBCT.

Influence on the Contrast-to-Noise Ratio (CNR)

In this study, the effect of slice thickness on contrast-to-noise ratio (CNR) was evaluated using both CT and CBCT imaging. The CNR was calculated with Pylinac for a low- contrast insert using a 7 mm × 7 mm ROI, with a background region placed directly beneath the insert. Slice thicknesses of 1, 3, and 5 mm were analyzed for each modality.

Referring to [Table 4], the outcomes indicate a notable positive relationship between slice thickness and contrast-to-noise ratio (CNR) in both CT and CBCT modalities. The CNR values for both imaging techniques improved as the slice thickness increased from 1 mm to 5 mm, owing to decreased image noise resulting from enhanced volume averaging.

In the case of CT, the CNR increased from 1.06 at 1 mm to 2.24 at 5 mm, reflecting considerable and stable improvement in low-contrast detectability. On CBCT, the CNR increased from 1.04 at 1 mm to 2.17 at 5 mm, but this enhancement was less pronounced. Interestingly, CBCT provided a slightly higher CNR than CT at 3 mm (1.99 vs. 1.67), although CT consistently had better results than CBCT at 1 mm and 5 mm slices.

These results support the conclusion that CNR improves with higher slice thickness, especially in CT, which performs better than CBCT for low-contrast detection at any slice thickness.

Impact of Slice Thickness on Dose Calculation in CT and CBCT

This section presents a comparative study of dose calculations performed in the Eclipse Treatment Planning System (TPS) using CT and CBCT images of the Catphan 604 phantom with varying slice thicknesses. The comparison was based on Dose-Volume Histograms (DVHs). To ensure consistency across DVH comparisons, the same contours were applied to each structure and for all studied slice thicknesses. The structures contoured in this study were the air, bone, and water. The slice thicknesses examined were 1, 3, and 5 mm. The RT plan consisted of four equally weighted box fields with beam energy of 6 MV [Figure 6].

Analysis of the RT plan conducted on both CBCT and CT images indicated that slice thickness had a minimal impact on dose distribution across all examined structures [Figure 7]. A comparative dosimetric evaluation between CT and CBCT imaging was performed through dose-volume histogram (DVH) analysis of the various structures, with a 5 mm slice thickness selected for this investigation [Figure 8].

Based on the obtained results, the DVH corresponding to air demonstrated perfect agreement, indicating that the imaging modality had no effect on dose deposition within the air structures. For water, a minor discrepancy existed between the CT and CBCT DVH curves, with CT exhibiting higher dose values. In the case of the bone, a more pronounced difference was observed between the two modalities.

Table 3: Noise and uniformity index value on HU for CT and CBCT images.

Slice Thickness (mm)	Imaging Modality	Average Noise Power	Uniformity Index
1 mm	CT CBCT	0.214 0.316	0.099 1.787
3 mm	CT CBCT	0.235 0.249	-0.197 1.896
5 mm	CT CBCT	0.232 0.304	-0.296 1.900

Table 4: CNR Values for CT and CBCT at Different Slice Thicknesses.

Slice Thickness (mm)	Imaging Modality	CNR
1 mm	CT CBCT	1.06 1.04
3 mm	CT CBCT	1.67 1.99
5 mm	CT CBCT	2.24 2.17

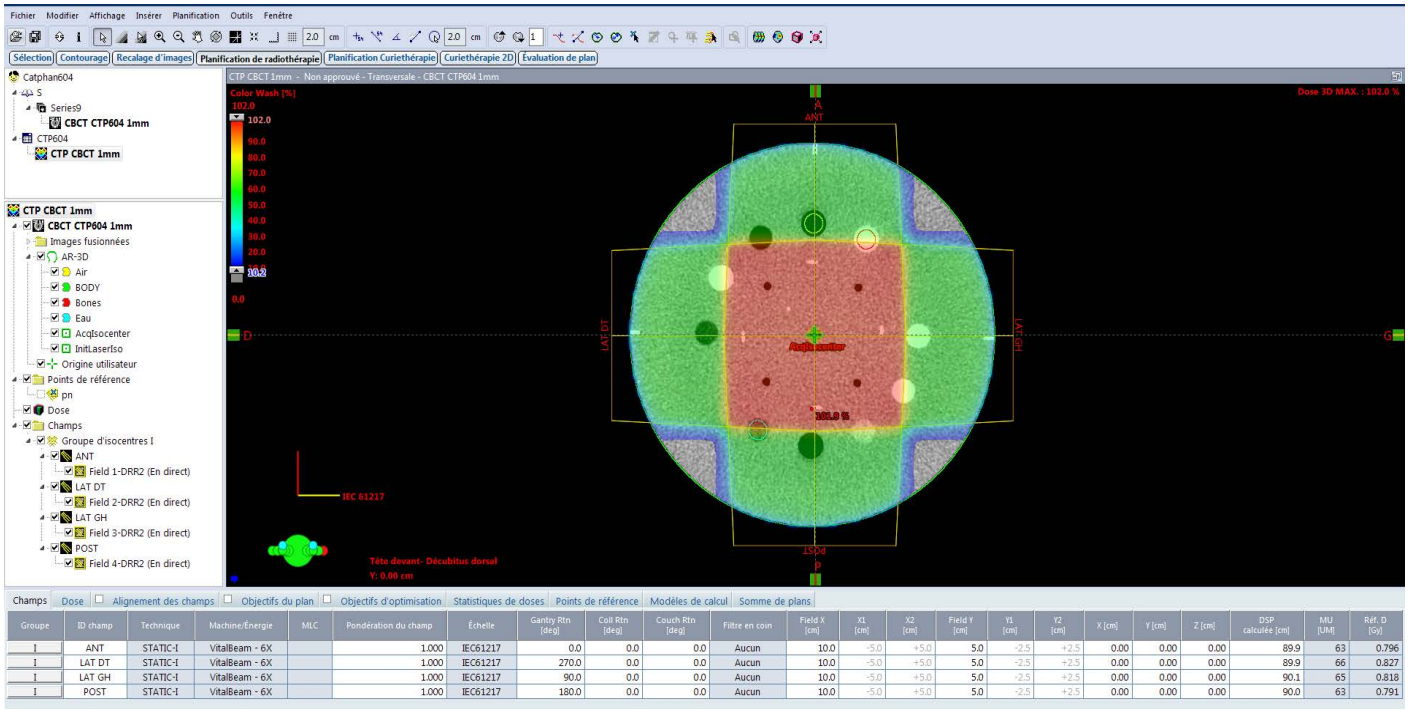

Groupe	ID champ	Technique	Machine/Énergie	MLC	Pondération du champ	Échelle	Gantry Rtn [deg]	Coll Rtn [deg]	Couch Rtn [deg]	Filtre en coin	Field X [cm]	X1 [cm]	X2 [cm]	Field Y [cm]	Y1 [cm]	Y2 [cm]	X [cm]	Y [cm]	Z [cm]	DSP calculée [cm]	MU [UM]	Ref. D [Gy]
1	ANT	STATIC-I	VitalBeam - 6X		1.000	IEC61217	0.0	0.0	0.0	Aucun	10.0	-5.0	+5.0	5.0	-2.5	+2.5	0.00	0.00	0.00	89.9	63	0.796
1	LAT DT	STATIC-I	VitalBeam - 6X		1.000	IEC61217	270.0	0.0	0.0	Aucun	10.0	-5.0	+5.0	5.0	-2.5	+2.5	0.00	0.00	0.00	89.9	66	0.827
1	LAT GH	STATIC-I	VitalBeam - 6X		1.000	IEC61217	90.0	0.0	0.0	Aucun	10.0	-5.0	+5.0	5.0	-2.5	+2.5	0.00	0.00	0.00	90.1	65	0.818
1	POST	STATIC-I	VitalBeam - 6X		1.000	IEC61217	180.0	0.0	0.0	Aucun	10.0	-5.0	+5.0	5.0	-2.5	+2.5	0.00	0.00	0.00	90.0	63	0.791

Figure 6: Visualization of dose distribution in Eclipse TPS for CBCT-based Catphan 604 phantom plan.

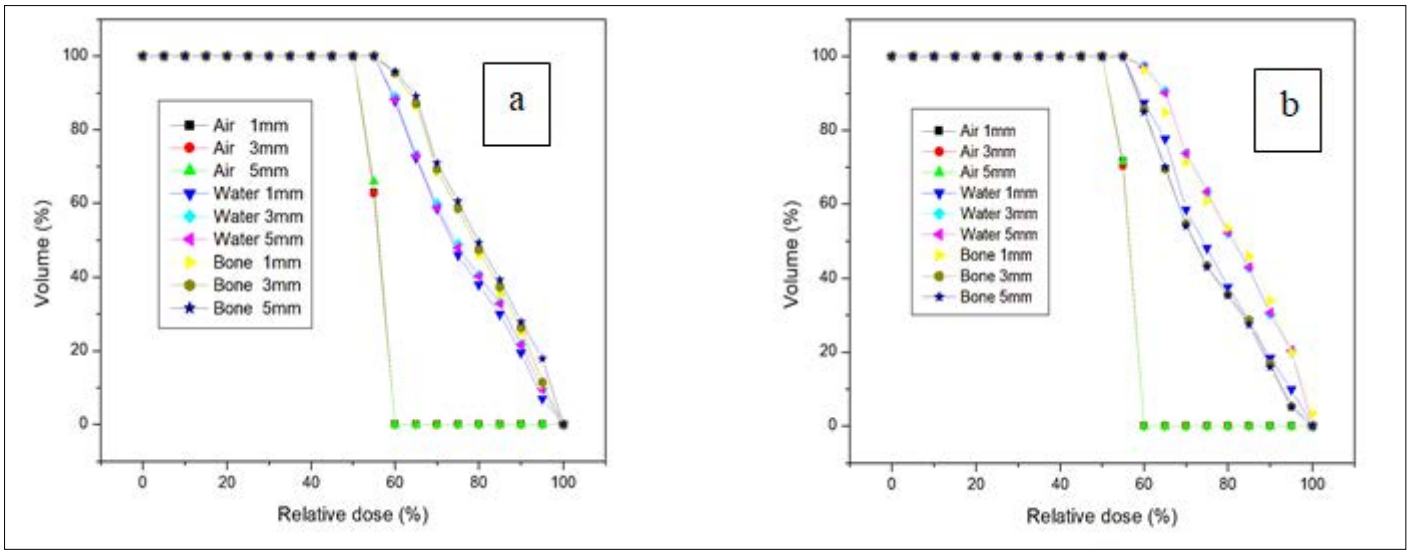

Figure 7: Influence of CT and CBCT slice thickness on DVH. **(a)** CBCT; **(b)** CT.

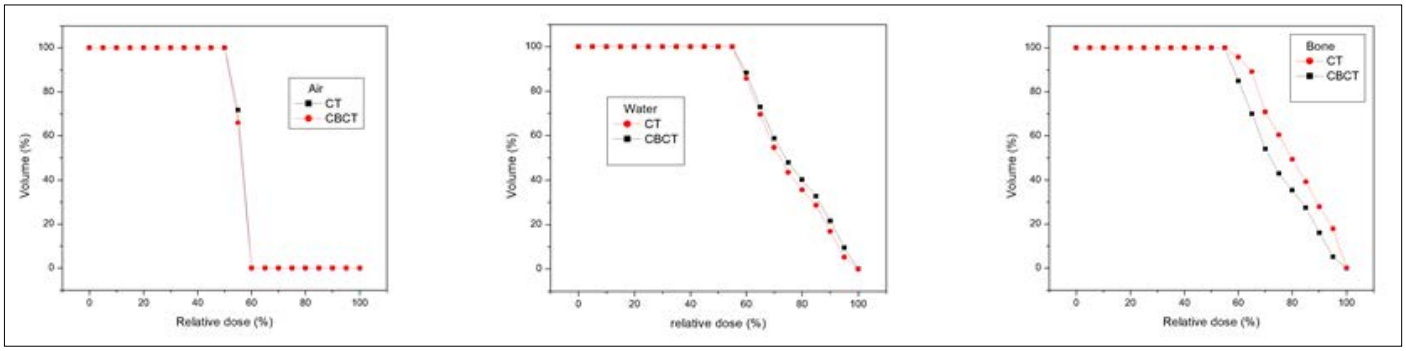

Figure 8: Comparison of DVHs for air, water, and bone structures on CT and CBCT images with a slice thick-ness of 5 mm.

DISCUSSION

This study highlights the significant influence of slice thickness on image quality parameters in computed to-mography (CT) and cone-beam computed tomography (CBCT) and its effect on RT dose calculation plans. The results demonstrate that thinner slices (1 mm) offer superior spatial resolution, facilitating precise visualization of fine anatomical details and small structures, making them particularly suitable for SRS and SRT. However, this improvement in resolution is accompanied by an increase in noise levels, which can complicate image interpretation. Conversely, thicker slices (3-5 mm) have a better signal-to-noise ratio, but at the expense of spatial resolution, making them more appropriate for larger target volumes in conventional techniques such as 3D-CRT. Comparative analysis between CT and CBCT revealed notable differences in image quality metrics, with CT consistently outperforming CBCT in terms of spatial resolution and contrast-to-noise ratio (CNR) across all slice thicknesses studied. Variations in Hounsfield Unit (HU) values between manufacturer-reported and measured values were also observed, particularly in CT images, with the differences increasing proportionally with the material density. Although CBCT exhibited more consistent HU values, its overall accuracy, particularly for high-density materials such as bone, was inferior to that of CT. Modulation transfer function (MTF) analysis demonstrated that, even with thicker slices, CT images provided superior spatial resolution compared to CBCT, a crucial aspect in RT planning, because the accuracy of target volume delineation is directly proportional to the accuracy of dose distribution. Furthermore, evaluation of the uniformity index and CNR showed that CT produces more consistent and reliable images, particularly in low-contrast situations, than CBCT. These results corroborate the findings of Chadwick et al. (2010), who demonstrated that variations in slice thickness and interslice intervals significantly influence the representation of normal anatomy and pathologies in CBCT images [15]. This study also aligns with the findings of Prabhakar et al. (2009), who identified that a CT slice thickness of 2.5 mm was optimal for tumor volumes less than 25 cc, while a thickness of 5 mm was more suitable for volumes greater than 25 cc [16]. Our observations regarding the impact of slice thickness on spatial resolution and noise levels are consistent with the results of Gaillandre et al. (2023) and McCollough et al. (2024), who found that using thinner slices (approximately 1 mm) generally improved the spatial resolution, facilitating the visualization of minute features and subtle anatomical changes [17, 18]. At the same time, the findings of this study on the limitations associated with thin slices are consistent with those of Diwakar and Kumar (2018) and Cruz-Bastida et al. (2019), who highlighted that this improvement in resolution was accompanied by increased complexity in image interpretation due to increased noise levels [19, 20]. The superiority of CT over CBCT in terms of HU accuracy, spatial resolution, and contrast-to-noise ratio, observed in our study, is consistent with the findings of Ronkainen et al. (2022) and Tran et al. (2021) [21, 22]. These authors also noted that CT is more suited to tasks requiring detailed tissue differentiation. Our observations on the limitations of CBCT, notably its increased susceptibility to artifacts and noise, are also consistent with the work of Sajja et al. (2020) and Bryce-Atkinson et al. (2021) [23, 24], who nevertheless highlighted the utility of CBCT in specific clinical applications, particularly when rapid on-site imaging is required. From a dosimetric perspective, the results obtained showed that the slice thickness did not have a significant influence on the dose distribution for all the structures studied. However, a comparison of the dose distribution between CT and CBCT showed that the difference between the two was observed for the bone, which is a denser element. This difference may be explained by the difference in HU values.

Technological advances in CBCT, such as iterative reconstruction algorithms and deep learning-based de-noising, bridge the performance gap with CT and improve its utility in RT, as suggested by Washio et al. (2020) and Kim et al. (2023) [25, 26]. Future research should explore the impact of advanced reconstruction algorithms on the image quality across various slice thicknesses and modalities. Moreover, investigating patient-specific factors influencing optimal slice thickness selection is crucial for adapting imaging protocols to various clinical situations, as highlighted by Estak et al. (2021) [27].

CONCLUSION

Our results indicate that slice thickness has a more significant impact on the overall image quality for CT and CBCT, where CT continuously achieved better spatial resolution and Hounsfield Unit accuracy. Thinner slices improve detail for high-precision techniques but result in increased noise, whereas larger slices reduce noise at the cost of resolution and are therefore better suited for larger targets. These findings highlight the importance of adapting slice thickness to individualized clinical needs, which may be optimized using new imaging meth-odologies. This knowledge will ultimately improve diagnostic accuracy and lead to more effective RT treat-ments for more patients.

The findings of this study will contribute to building a practical framework for implementing open-source solu-tions within normal clinical workflows to enhance diagnostic accuracy and optimize RT treatment planning. This research fills an important gap in the literature by demonstrating the utility of open-source tools to improve patient outcomes and elevate the standard of care for patients receiving RT.

STATEMENTS & DECLARATIONS

Authorship Statement

All authors have read and approved the final version of the manuscript. They agree with the content, data accuracy, and presentation, and consent to its submission for publication. Each author contributed significantly to the work and accepts responsibility for its integrity.

FUNDING

The authors declare that no funds, grants, or other support were received during the preparation of this manuscript.

COMPETING INTERESTS

The authors have no relevant financial or non-financial interests to disclose.

AUTHOR CONTRIBUTIONS

All authors contributed to the study conception and design.

ETHICS APPROVAL

Ethical approval was not required for this study, as the data were obtained from a physical phantom and did not involve human or animal subjects.

CONSENT TO PARTICIPATE

not applicable. The study involved only phantom data, and no human participation.

CONSENT TO PUBLISH

Not applicable. This study was based solely on phantom data and does not involve any individual subject data.

DATA AVAILABILITY

the data supporting the findings of this study are available from the corresponding author upon reasonable request.

REFERENCES

1. Davis AT, Palmer AL, Nisbet A. Can CT scan protocols used for radiotherapy treatment planning be adjusted to optimize image quality and patient dose? A systematic review. The British journal of radiology. 2017; 90: 20160406.
2. Thorwarth D. Functional imaging for radiotherapy treatment planning: current status and future directions-a review. The British journal of radiology. 2015; 88: 20150056.
3. Zaffino P, Raggio CB, Thummerer A, Marmitt GG, Langendijk JA et al. Toward Closing the Loop in Image-to-Image Conversion in Radiotherapy: A Quality Control Tool to Predict Synthetic Computed Tomography Hounsfield Unit Accuracy. Journal of Imaging. 2024; 10: 316.
4. Grégoire V, Guckenberger M, Haustermans K, Lagendijk JJ, Ménard C, et al. Image guidance in radiation therapy for better cure of cancer. Molecular oncology. 2020; 14: 1470-1491.
5. Issa J, Riad A, Olszewski R, Dyszkiewicz-Konwińska M. The Influence of Slice Thickness, Sharpness, and Contrast Adjustments on Inferior Alveolar Canal Segmentation on Cone-Beam Computed Tomography Scans: A Retrospective Study. Journal of Personalized Medicine. 2023; 13: 1518.
6. Lee JH. Comparison of thin-slice CT and conventional CT for lung cancer detection. The American Journal of Radiology. 2015; 204: 637-643.
7. Kim JH. Evaluation of noise and image quality in CT with different slice thicknesses. Journal of Applied Clinical Medical Physics. 2017; 18: 55-63.
8. Wang X. Effect of slice thickness on image quality in CT. Journal of Medical Imaging and Health Informatics. 2018; 8: 1057-1062.
9. Purdy JA, Smith AR. Three-dimensional Photon Treatment Planning: Report of the Collaborative Working Group on the Evaluation of Treatment Planning for External Photon Beam Radiotherapy. Pergamon Press. 1991.
10. Ezzell GA, Galvin JM, Low D, Palta JR, Rosen I, et al. Guidance document on delivery, treatment planning, and clinical implementation of IMRT: report of the IMRT Subcommittee of the AAPM Radiation Therapy Committee. Medical physics 2003; 30: 2089-2115.
11. Halvorsen PH, Cirino E, Das IJ, Garrett JA, Yang J, et al. AAPM-RSS medical physics practice guideline 9. a. for SRS-SBRT. Journal of applied clinical medical physics. 2017; 18: 10-21.
12. https://static1.squarespace.com/static/5367b059e4b05a1adcd295c2/t/5efe3c9cb415005eed8ae334/1593719971234/CTP604Manual20200701.pdf
13. Kerns JR. Pylinac: Image analysis for routine quality assurance in radiotherapy. Journal of Open Source Software. 2023; 8: 6001.
14. Wu RY, Liu AY, Williamson TD, Yang J, Wisdom PG, et al. Quantifying the accuracy of deformable image registration for cone-beam computed tomography with a physical phantom. Journal of applied clinical medical physics. 2019; 20: 92-100.
15. Chadwick JW, Lam EW. The effects of slice thickness and interslice interval on reconstructed cone beam computed tomographic images. Oral Surgery, Oral Medicine, Oral Pathology, Oral Radiology, and Endodontology. 2010; 110: e37-e42.
16. Prabhakar R, Ganesh T, Rath GK, Julka PK, Sridhar PS, et al. Impact of different CT slice thickness on clinical target volume for 3D conformal radiation therapy. Medical dosimetry. 2009; 34: 36-41.
17. Gaillandre Y, Duhamel A, Flohr T, Faivre JB, Khung S, et al. Ultra-high resolution CT imaging of interstitial lung disease: impact of photon-counting CT in 112 patients. European Radiology. 2023; 33: 5528-5539.
18. McCollough CH, Winfree TN, Melka EF, Rajendran K, Carter RE, et al. Photon-Counting Detector Computed Tomography Versus Energy-Integrating Detector Computed Tomography for Coronary Artery Calcium Quantitation. Journal of computer assisted tomography. 2024; 48: 212-216.
19. Diwakar M, Kumar M. A review on CT image noise and its denoising. Biomedical Signal Processing and Control. 2018; 42: 73-88.
20. Cruz-Bastida JP, Zhang R, Gomez-Cardona D, Hayes J, Li K, et al. Impact of noise reduction schemes on quantitative accuracy of CT numbers. Medical Physics. 2019; 46: 3013-3024.
21. Ronkainen AP, Al-Gburi A, Liimatainen T, Matikka H. A dose–neutral image quality comparison of different CBCT and CT systems using paranasal sinus imaging protocols and phantoms. European Archives of Oto-Rhino-Laryngology. 2022 ; 279: 4407-4414.
22. Tran TTN, Jin DSC, Shih KL, Hsu ML, Chen JC. An image quality comparison study between homemade and commercial dental cone-beam CT systems. Journal of Medical and Biological Engineering. 2021; 41: 870-880.
23. Sajja S, Lee Y, Eriksson M, Nordström H, Sahgal A, et al. Technical principles of dual-energy cone beam computed tomography and clinical applications for radiation therapy. Advances in radiation oncology. 2020; 5: 1-16.
24. Bryce-Atkinson A, De Jong R, Marchant T, Whitfield G, Aznar MC, et al. Low dose cone beam CT for paediatric image-guided radiotherapy: Image quality and practical recommendations. Radiotherapy and Oncology. 2021; 163: 68-75.
25. Washio H, Ohira S, Funama Y, Morimoto M, Wada K, et al. Metal artifact reduction using iterative CBCT reconstruction algorithm for head and neck radiation therapy: a phantom and clinical study. European Journal of Radiology. 2020; 132: 109293.
26. Kim K, Lim CY, Shin J, Chung MJ, Jung YG. Enhanced artificial intelligence-based diagnosis using CBCT with internal denoising: Clinical validation for discrimination of fungal ball, sinusitis, and normal cases in the maxillary sinus. Computer Methods and Programs in Biomedicine. 2023; 240: 107708.
27. Estak K, Mohammadzadeh M, Gharehaghaji N, Mortezazadeh T, Khatyal R, et al. Optimisation of CT scan parameters to increase the accuracy of gross tumour volume identification in brain radiotherapy. Journal of Radiotherapy in Practice. 2021; 20: 340-344.